Bull. Chem. Soc. Jpn., 73, 785—793 (2000)

Electron-Transfer Process in Layered Photoreceptors Containing Azo Compounds

Tomoyuki Shimada, Masaomi Sasaki, Tamotsu Aruga, and Minoru Umeda[*,†,#]

Imaging Technology Division, Ricoh Company, Ltd., 16-1 Honda-machi, Numazu 410-0004

†Research & Development Center, Ricoh Company, Ltd., 16-1 Shinei-cho, Tsuzuki-ku, Yokohama 224-0035

(Received April 8, 1999)

Photoinduced electron transfer (ET) is the most essential process for carrier photogeneration in organic optoelectronic devices. In azo compound-based layered photoreceptors, carrier photogeneration is sensitized by hole transport material (HTM) incorporation. We investigated this process to elucidate the highly sensitizing mechanism. First, the photoinduced ET efficiency and overall quantum efficiency were measured and compared for the layered photoreceptor and the carrier generation layer. The result that the HTM enhances the photoinduced ET implies that the HTM works catalytically to diminish the activation energy. Although such extrinsic ET takes place independently of an electric field, the subsequent geminate pair dissociation depends on the electric field. Next, the energy-gap dependence of the ET was investigated by employing more than 50 photoreceptors to vary the energy gap over a wide range. The measured efficiency was plotted against the energy gap, in which an inverted region was not observed.

Organic photoreceptors have a light-to-electrical energy conversion efficiency[1,2] larger than 0.5, which is remarkable when compared to the efficiency of other organic devices.[3] Generally, the carrier photogeneration efficiency in inorganic compounds exceeds that of organic compounds, because free carriers are directly generated by photon absorption in inorganic materials (crystals),[4] whereas photocarriers are generated via two-step reactions in organic compounds.[5] An exciton produced by photon absorption generates a geminate hole-electron pair, which then dissociates into free carriers:[6]

$$M_1^* + M_2 \rightarrow (M_1^- \cdots M_2^+) \rightarrow M_1^- + M_2^+ \quad (1)$$

The tightly bound states of the hole and electron, the exciton and geminate pair, are difficult to separate against the Coulomb energy. In addition, a multistep reaction usually reduces the overall efficiency. For these reasons, adequate comprehension of the carrier photogeneration mechanism with high-efficiency photoreceptors is required to understand organic and optoelectronic devices.

Phthalocyanines (Pcs) and azo compounds are known to be highly photosensitive materials. In Pcs, photocarriers are intrinsically generated in Pc molecules.[7] The former reaction, represented in Eq. 1, strongly depends on the electric field; whereas the latter reaction is faster than the former,[7] making it difficult to analyze. However, photocarrier generation in azo compounds-based layered photoreceptor occurs extrinsically between the azo compound and the hole transport material (HTM) involved.[8] In this system, the reaction steps could be studied independently, because the preceding reaction is rate determining in a strong electric field and the following is rate determining in a weak electric field.

In this paper, we focus on the extrinsic photocarrier generation of layered photoreceptors containing various azo compounds in order to elucidate the basic nature of the two significant reactions. First, the overall reactions of the photoreceptors are reviewed, and the two reactions are concisely characterized. The preceding reaction in Eq. 1, photoinduced electron transfer (ET), is distinguished by the energy gap between the initial and final states. Next, more than 50 photoreceptors were prepared using 3 azo compounds in combination with 26 HTMs (*N,N*-diphenyl-4-biphenylylamine derivatives)[9] in order to vary the energy gap over a wide range. The energy-gap dependence of the reaction efficiency was measured, analyzed and then compared with that of oxo(phthalocyaninato)titanium(IV) (TiOPc).

Experimental

Materials. Azo compounds (Azo–FO, Azo–TPA, and Azo–DSB) and HTMs (APS-1 and APS-2) were obtained as commercial sources for organic photoreceptors from Ricoh Co., Ltd (see Fig. 1). The *N,N*-diphenyl-4-biphenylylamine derivatives (HTMs) shown in Table 1 were prepared by modifying the Ullmann reaction. Commercially available solvents and reagents were used without further purification. Column chromatography was carried out on a Wakogel C-300 (Wako Pure Chemical Industries, Ltd.). All melting points are uncorrected. Elemental analyses were performed with a Yanako CHN Corder MT-5. Poly(vinyl butyral) was obtained from Sekisui Chemical Co., Ltd. as S-Lec. Polycarbonate was obtained from Teijin Kasei Limited as Panlite. Both polymers were used without purification.

Synthesis of *N,N*-Di(*p*-tolyl)-4′-methyl-4-biphenylylamine

Present address: Department of Applied Chemistry, Graduate School of Engineering, Tohoku University, Aramaki Aoba 07, Aoba-ku, Sendai 980-8579, Japan.

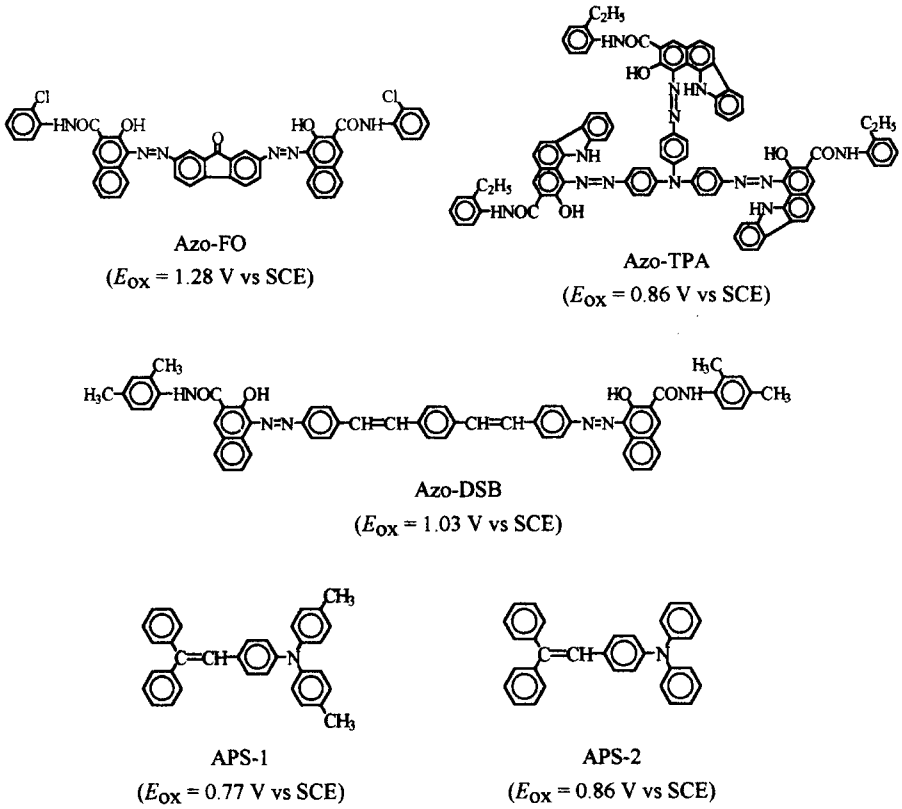

Fig. 1. Chemical structures of azo compounds (Azo–FO, Azo–TPA, and Azo–DSB) and hole transport materials (APS-1 and APS-2).

(9): A mixture of 4-iodo-4′-methylbiphenyl (3.38 g, 11.5 mmol), di(*p*-tolyl)amine (2.27 g, 11.5 mmol), potassium carbonate (1.67 g, 12.1 mmol), and copper powder (50 mg) in nitrobenzene (50 ml) was stirred under nitrogen at 205—208 °C for 11 h. The reaction mixture was then cooled to room temperature, and filtered with celite. After water was added to the filtrate, nitrobenzene was removed under reduced pressure. The residue was extracted with toluene, washed with water, dried over magnesium sulfide, and evaporated. The resulting compound was chromatographed on silica gel with 5 : 1 (v/v) toluene-hexane as the eluent to give **9**. Recrystallization of the product from ethanol gave colorless needles (2.08 g, 49.6%), mp 118.0—119.0 °C. Found: C, 88.97; H, 6.84; N, 3.65%. Calcd for $C_{27}H_{25}N$: C, 89.21; H, 6.93; N, 3.86%.

Synthesis of *N*-(4′-Methylbiphenyl-4-yl)-*N*-(*p*-tolyl)-4′-methyl-4-biphenylylamine (14): A mixture of 4-iodo-4′-methylbiphenyl (8.82 g, 30.0 mmol), *p*-toluidine (1.61 g, 15.0 mmol), potassium carbonate (6.22 g, 45.0 mmol), and copper powder (0.48 g) in nitrobenzene (60 ml) was stirred under nitrogen at 210—211 °C for 20 h. The reaction mixture was then cooled to room temperature, and filtered with celite. After water was added to the filtrate, nitrobenzene was removed under reduced pressure. The residue was extracted with diethyl ether, washed with water, dried over magnesium sulfide, and evaporated. The resulting compound was chromatographed on silica gel with 3 : 1 (v/v) toluene–hexane as the eluent to give **14**. Recrystallization of the product from ethyl acetate–ethanol gave colorless needles (1.76 g, 26.7%), mp 147.0—148.0 °C. Found: C, 90.28; H, 6.69; N, 3.02%. Calcd for $C_{33}H_{29}N$: C, 90.16; H, 6.65; N, 3.19%.

Quantum Efficiency. The procedure for preparing the layered photoreceptor was as follows: A tetrahydrofuran (THF) dispersion containing the poly(vinyl butyral) and azo compound in a weight ratio of 4 : 10 was prepared using a ball mill. The dispersion was applied to the surface of an aluminized polyester film using a roller coater and then dried for three minutes at 120 °C under atmospheric conditions to form the carrier generation layer (CGL) with a 0.1—0.5 μm thickness. A THF solution containing bisphenol-A–polycarbonate and HTM was applied to the surface of the CGL using a blade, and then dried for twenty minutes at 120 °C under atmospheric conditions to form a carrier transport layer (CTL) 10—30 μm thick. Unless otherwise stated, the weight ratio of HTM : polycarbonate was 9 : 10 and the solids content of the solution was kept at 11 wt%. Thus, the desired layered photoreceptors were prepared.

The quantum efficiency of photocarrier generation in the layered photoreceptors was measured by a xerographic technique.[10,11] This method enabled us to measure the surface potential on the photoreceptor activated by a negative corona charge under illumination. The application of corona charge and subsequent exposure of the photoreceptor to light were conducted in an electrostatic paper analyzer (Kawaguchi Electric Works; SP-428), which consisted of a corona generating unit, a tungsten lamp as a light source and an electrostatic voltmeter. Monochromatic light was applied to the CGL of the layered photoreceptor through an optically transparent CTL. The photoinduced discharge curve leads to a quantum efficiency (ϕ), which represents the number of surface charges removed by each absorbed photon,[11]

$$\phi(F) = \frac{C}{e \cdot J}\left|\frac{dV_s}{dt}\right|_F. \quad (2)$$

Here, C is the capacitance of the photoreceptor per unit area, e is the electronic charge, J is the incident photon flux (absorbed photons in CGL per second and per unit area), V_s is the surface potential, and F is the electric field. During this series of experiments, the secondary light component at shorter wavelengths was eliminated

Table 1. *N,N*-Diphenyl-4-diphenylylamine Derivatives Used in Carrier Transport Layers

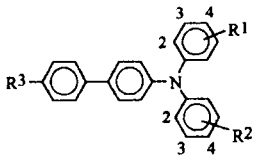

No.	R^1	R^2	R^3	Yield	Mp	Elemental analysis (%) Obsd (Calcd)			E_{ox}
				%	°C	C	H	N	V vs. SCE
1	4-OCH_3	4-OCH_3	OCH_3	34.4	116.0—117.5	78.50 (78.81)	5.98 (6.12)	3.35 (3.40)	0.630
2	4-OCH_3	4-OCH_3	C_2H_5	24.4	129.0—129.5	81.94 (82.11)	6.67 (6.66)	3.26 (3.42)	0.640
3	4-OCH_3	4-OCH_3	*t*-C_4H_9	18.4	89.5—100.5	82.39 (82.33)	7.14 (7.15)	3.22 (3.20)	0.660
4	4-OCH_3	4-OCH_3	CH_3	31.6	113.5—114.0	81.95 (81.98)	6.38 (6.38)	3.35 (3.54)	0.660
5	4-OCH_3	4-OCH_3	H	21.0	129.5—130.5	81.57 (81.86)	5.85 (6.08)	3.58 (3.67)	0.670
6	4-OCH_3	4-CH_3	CH_3	27.1	94.0—95.0	85.46 (85.45)	6.64 (6.64)	3.5 (3.69)	0.720
7	4-CH_3	4-CH_3	OCH_3	43.3	142.5—143.5	85.59 (85.45)	6.71 (6.64)	3.80 (3.69)	0.765
8	4-OCH_3	H	CH_3	34.8	103.5—104.5	85.14 (85.45)	6.13 (6.34)	3.73 (3.83)	0.770
9	4-CH_3	4-CH_3	CH_3	49.6	118.0—119.0	88.97 (89.21)	6.84 (6.93)	3.65 (3.86)	0.785
10	4-CH_3	4-CH_3	C_2H_5	50.5	87.0—88.0	89.24 (89.08)	7.29 (7.21)	3.49 (3.71)	0.795
11	4-CH_3	4-CH_3	*t*-C_4H_9	29.5	101.0—103.0	88.99 (88.84)	7.56 (7.71)	3.58 (3.45)	0.800
12	4-CH_3	4-(*p*-$C_2H_5C_6H_4$)	C_2H_5	44.9	125.0—126.0	90.08 (89.89)	7.18 (7.11)	2.87 (3.00)	0.805
13	4-CH_3	4-CH_3	H	59.9	129.5—130.5	89.28 (89.36)	6.72 (6.63)	3.85 (4.01)	0.815
14	4-CH_3	4-*p*-tolyl	CH_3	26.7	147.0—148.0	90.28 (90.16)	6.69 (6.65)	3.02 (3.19)	0.815
15	3-CH_3	3-CH_3	OCH_3	58.7	102.5—103.5	85.49 (85.45)	6.43 (6.64)	3.59 (3.69)	0.830
16	4-CH_3	H	CH_3	49.7	87.5—89.5	89.49 (89.36)	6.30 (6.63)	3.88 (4.01)	0.835
17	3-CH_3	3-CH_3	*t*-C_4H_9	53.4	90.5—93.5	88.78 (88.84)	7.81 (7.71)	3.75 (3.45)	0.840
18	3-CH_3	3-CH_3	C_2H_5	62.6	123.5—124.5	89.33 (89.08)	7.40 (7.21)	3.51 (3.71)	0.850
19	H	H	OCH_3	26.0	132.5—133.5	85.42 (85.44)	5.96 (6.02)	3.98 (3.99)	0.855
20	3-CH_3	3-CH_3	CH_3	53.0	111.0—112.0	89.37 (89.21)	6.74 (6.93)	3.66 (3.86)	0.860
21	3-CH_3	3-CH_3	H	61.6	104.5—105.5	89.48 (89.36)	6.71 (6.63)	3.76 (4.01)	0.880
22	4-CH_3	H	H	40.9	96.0—98.0	89.64 (89.51)	6.30 (6.31)	3.92 (4.18)	0.880
23	H	H	CH_3	39.7	104.0—105.0	89.27 (89.51)	6.10 (6.31)	4.02 (4.18)	0.890
24	H	H	*t*-C_4H_9	54.4	124.5—125.0	89.19 (89.08)	6.92 (7.21)	3.63 (3.71)	0.890
25	H	H	H	56.7	111.0—111.5	89.70 (89.67)	5.79 (5.97)	4.21 (4.36)	0.910
26	H	H	C_2H_5	24.0	94.0—95.0	89.23 (89.34)	6.49 (6.65)	3.81 (4.01)	0.945

using a sharp-cut filter. The light power for exposure was measured by a photometer (Tektronix; J16).

Absorption and Photoluminescence Spectra. A single-layer CGL or layered CGL/CTL was set on the surface of nonfluorescent quartz glass. The above-prepared dispersion was applied to one side of the quartz glass using a dip-coating process to form the CGL. To form a layered CGL/CTL, a CTL-coating solution was applied in the same manner as described above to the surface of the CGL. This produced a CTL, 20 μm thick. In either case, the CGL was about 0.15 μm thick.

The absorption spectra of the CGL were obtained using a spectrophotometer (Shimadzu; UV-3100). The photoluminescence (PL) spectra of these samples were measured using an intensifier multichannel photodetector (Otsuka Electronics; IMUC-7000) and an argon-ion laser (488.1 nm—200 μW) as a continual excitation source. The photodetector for this instrument was a photodiode array in combination with an image-intensifier tube. The photodetector was protected from the exciting light by a 560 nm short-wavelength cut-off filter. Luminescence from the CGL was measured eight times in the range of 650—900 nm with a sampling time of 200 ms, and then averaged to improve the S/N ratio.

Electron Transfer Efficiency. The PL intensities of the layered CGL/CTL and the single-layer CGL were compared. The PL quenching phenomenon is based on ET from the HTM in the ground state to the photoexcited azo compound.[12] Since the measured PL intensities were obtained under the same azo compound content and the same excitation-light power, the ET efficiency (ϕ_{et}) can be expressed by[12]

$$\phi_{et} = 1 - I_{GT}(0)/I_G(0). \quad (3)$$

Here, $I_{GT}(0)$ and $I_G(0)$ denote the PL intensities for the layered CGL/CTL and the single-layer CGL, respectively.[12]

PL with an applied electric field was measured by the same apparatus as that used in the case of measurement without an electric field. The layered CGL/CTL and the single-layer CGL with electrodes were formed in the following manner. The above-discribed CGL (0.15 μm thickness) and CTL (2.0 μm thickness) were applied to the surface of an indium tin oxide (ITO)-coated polyester substrate. In addition, on the surface of the CTL or CGL, an aluminum electrode was evaporated to a thickness of 200 Å and a diameter of 8 mm to serve as a counter electrode.

A laser beam used for excitation was spread out ca. 30 times by a beam expander (632.8 nm—1.0 Wm^{-1}). The excitation light was applied to the semi-transparent aluminum side through a 6 mm caliber mask, and the luminescence was observed from the ITO side.

The PL spectra of the single-layer CGL were measured with an applied potential of 0—120 V between the ITO electrode and the aluminum electrode using a dc voltage source, so that the ITO electrode would have a positive potential.

Therefore, the ET efficiencies with an applied electric field of E are given as

$$\phi_{et}(E) = 1 - I_{GT}(E)/I_G(0), \quad (4)$$

where $I_{GT}(E)$ is the PL intensity for the layered CGL/CTL measured at an electric field of E; $I_G(0)$ is the PL intensity for the single-layer CGL at zero field.

The ET efficiencies for the single-layer CGL with an applied electric field, are expressed by[7]

$$\phi_{et}(E) = 1 - I_G(E)/I_G(0), \quad (5)$$

where $I_G(E)$ is the PL intensity for the single-layer CGL measured at an electric field of E.

Electroabsorption of Azo Compounds. Samples for the measurement of electroabsorption (EA) spectra were prepared as follows. The dispersions were applied to an indium tin oxide (ITO)-coated glass using a dip-coating technique to form an azo compound layer of about 0.1 μm thick. A semi-transparent aluminum electrode was vacuum-deposited to a thickness of about 150 Å to serve as a counter electrode. Monochromatic light from a 150 W halogen lamp was focused onto this sandwiched cell through a monochromator (Nikon; P250). Light passing through the cell was focused on a p-i-n Si photodiode (Hamamatsu Photonics; S3072). A 1 kHz square voltage was applied to the sample cell, so that the aluminum electrode would have a positive potential. The electrical signal derived from the photodiode was fed to a lock-in amplifier (NF Electronic Instruments; LI-575) for measuring the difference in the light intensity transmitted by the sample (ΔI) with the operation at 2 kHz (2f mode). The signal from the photodiode was directly measured for evaluating the total transmitted light intensity (I). In this measurement, the obtained data satisfied the relationship[13,14]

$$\Delta I/I = -d \cdot \Delta\alpha, \quad (6)$$

where d is the thickness of the pigment layer and $\Delta\alpha$ is the modulation amplitude of the absorption coefficient.

Ionization Potential and Oxidation Potential Measurements. The ionization potentials of azo compounds and HTMs were measured for the single-layer CGL and the single-layer CTL using photoelectron emission spectroscopy (Riken Keiki Co.; AC-1).[15] The first oxidation half-wave potentials (E_{ox}) of the HTMs were measured by cyclic voltammometry in an acetonitrile solution containing 0.1 mol dm^{-3} tetraethylammonium perchlorate as a supporting electrolyte and 5×10^{-3} mol dm^{-3} HTM. A platinum disc, platinum foil and SCE were used as the working, counter and reference electrodes, respectively. The E_{ox} of azo compounds were also measured by cyclic voltammometry using the dispersion in an acetonitrile solution.[16,17]

Measurement of Sample Thickness. The thickness of the photoreceptors was measured by a surface-profile measuring system (Sloan; Dektak IIA).

All measurements were carried out at 25±2 °C.

Results and Discussion

Photocarrier Generation Between Azo Compound and Hole Transport Material. The plots in Fig. 2 show the overall quantum efficiencies (ϕ) and photoinduced ET efficiencies (ϕ_{et}) of a layered photoreceptor containing Azo–FO in the CGL and APS-1 in the CTL, and a single-layer CGL (without CTL). Both the overall quantum efficiency of the layered photoreceptor and that of the single-layer CGL are independent of their thickness. In other words, the carrier-transport process in the layered photoreceptor and the single-layer CGL are not affected by the thickness.[10,18,19] For this reason, the photoinduced discharge in the photoreceptor and that in the single-layer CGL are both considered to be governed by the emission-limited conditions.[20] Furthermore, no residual potential was observed in either the layered photoreceptor or the single-layer CGL after they were sufficiently exposed to light, so that the value of the carrier transport efficiency can be taken as 1. Therefore, the overall efficiency of photocarrier generation represented by Eq. 1 is conventionally expressed as[21]

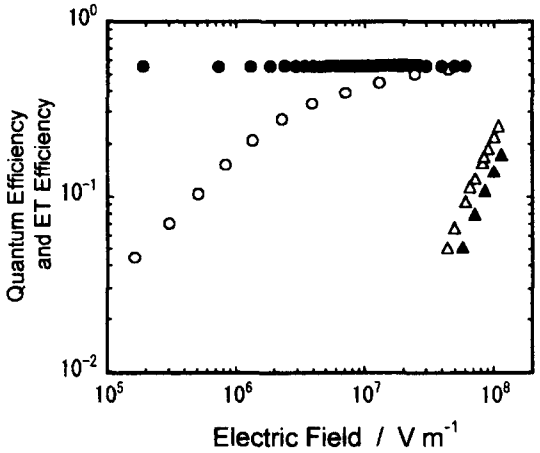

Fig. 2. The electric field dependence of the ET efficiencies (filled symbols) and the quantum efficiencies (open symbols) of layered photoreceptor (circles) and single-layer CGLs (triangles), all using Azo–FO in the CGL and using APS-1 in the CTL.

$$\phi = \phi_{et} \times \phi_{diss}. \quad (7)$$

Here, ϕ_{diss} is the efficiency of geminate pair dissociation into free carriers.

When the photoinduced ET efficiency of layered photoreceptor is compared to that of a single-layer CGL, the magnitude of the former is known to exceed that of the latter from Fig. 2. This result indicates that the CTL extrinsically sensitizes the photoinduced ET efficiency; in other words, a number of ET reactions occur between a photoexcited azo compound and HTM. As shown in Fig. 3, the ET site is not a planar CGL/CTL interface, but the CGM/HTM interface on the CGM particle, which is caused by penetration of HTM from the CTL during the coating procedure.[19,22] Moreover, it has been experimentally confirmed that the HTM and CGM ratio in CGL of the layered photoreceptor is nearly the same weight.[22] From this composition, the CGL bulk of the layered photoreceptor is thought to be almost a homogeneous structure.[23] Since the rate constant is independent of the distance between the HTM and CGM molecules, the ET is considered to be an adiabatic reaction.[23] This implies that the overlap of the molecular orbital of the reactants is large; thus, the electron clouds of the reacting molecules are thought

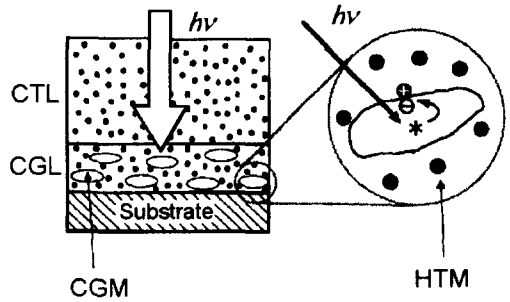

Fig. 3. Schematic representation of the photocarrier generation at CGM/HTM interface, which appeared as a result of HTM penetration during the CTL coating. Astaisk (*) means photoexcited CGM.

to spread according to the π-electron conjugated molecular structures, and that the reactants in the CGL bulk are at a high concentration. Since, it is known that the exciton diffusion is much faster than the subsequent processes, this diffusion is not a rate-determining step throughout the photocarrier generation process.[24] These results explain that the ET efficiency of the layered photoreceptor is much higher than that of the single-layer CGL.

As for the single-layer CGL, the photoinduced ET efficiency and overall efficiency strongly depended on the electric field. The overall efficiency was slightly higher than the ET efficiency. Concerning this case, we can not deny the extrinsic ET by a small amount of impurities (donor or acceptor) when we consider Ref. 25. However, because the slopes of both efficiencies increased monotonically and showed a linear correlation, this reaction is considered to be the intrinsic ET (same as Pcs)[7] rather than the extrinsic ET between Azo and the impurities. Accordingly, in the single-layer CGL, the preceding ET to generate geminate pairs by photoexcitation is considered to be rate determining, and the subsequent dissociation can be taken to occur with an efficiency of ca. 1.

For the layered photoreceptor, the ET efficiency was almost independent of the electric field; however, the overall efficiency depended on the electric field, the magnitude of which approached that of the ET efficiency at a high electric field strength. From these observations, it is clear that (i) the preceding ET enhanced by a HTM restrains the overall efficiency at a higher electric field, and (ii) the subsequent geminate-pair dissociation is diminished at a lower electric field.

Figures 4a and 4b, respectively, show the illumination wavelength dependence of the photoinduced ET and the overall quantum efficiencies of the layered photoreceptor, obtained as described above. The result that the ET efficiency remained constant when the illumination wavelength was shifted confirms that the photoexcited state of an azo compound relaxes to the lowest excited state, and then interacts with the HTM.[18] The overall photocarrier generation efficiency is also known to be independent of the illumination wavelength, as can be seen in Fig. 4b. This implies that the geminate pair dissociation reaction is also not influenced by the excitation photon energy.

Figures 5a and 5b show the electroabsorption (EA) spectra of the single-layer CGL and the CGL/CTL layered sample, respectively. The EA spectral profile of the single CGL is in good agreement with that of the first derivative of the absorption (A) in terms of the photon energy (E). Because of this agreement, the azo compound produces a Frenkel exciton by photon absorption. This consideration is supported by the azo compound PL lifetime of 116 ps. In general, Frenkel exciton, which is regarded as the first excited singlet state (S_1) or lowest triplet state (T_1), is hard to dissociate because the hole and electron are tightly bound in a molecule. For this reason, exciton in the single-layer CGL produces little ET to generate the geminate pair. As for the CGL/CTL layered structure, the electroabsorption spectrum also indicates the

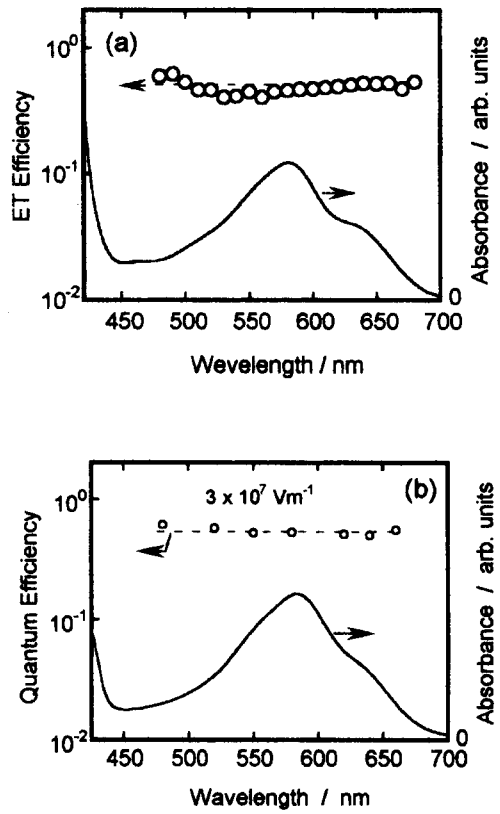

Fig. 4. Dependence of illumination wavelength on the ET efficiency (a) and the quantum efficiency (b) in Azo–FO-based layered photoreceptor. The absorption in the region shorter than 460 nm is attributed to APS-1 used in the CTL.

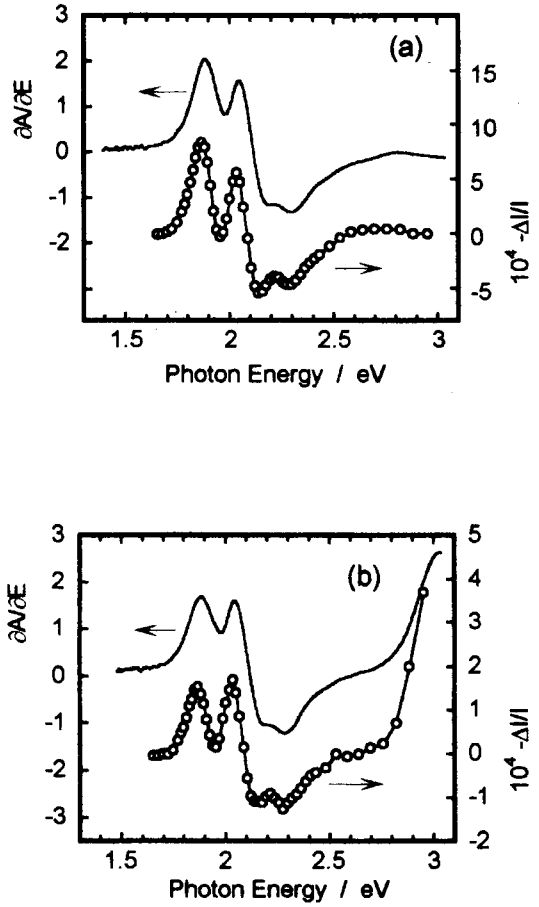

Fig. 5. EA spectra of Azo–FO sample (a) and Azo–FO/APS-1 layered sample (b). The first derivative of the absorbance (A) with respect to photon energy (E) is also shown. The absorption above 2.8 eV in (b) is attributed to APS-1.

existence of the Frenkel exciton. From this observation, it is concluded that the Frenkel exciton of the azo compound, which is also produced in the layered structure, makes ET more easily with the existence of HTM.

According to the above results, schematic photocarrier generation diagrams of single-layer CGL and layered photoreceptor are represented in Fig. 6. The photoexcited azo compound relaxes to the Frenkel exciton, in this case S_1, the hole-electron pair of which is tightly bound by the Coulomb force. Therefore, a comparatively large activation energy would be required to cause ET between the neighboring azo molecules, because the energy levels of the initial and final states are the same as shown in Fig. 6 (left side). In contrast, HTM of the layered photoreceptor is thought to diminish the activation energy catalytically, allowing ET to occur more easily (Fig. 6 right side).[9] However, the product of photoinduced ET, the geminate pair, is not yet a free carrier; external energy from the electric field is apparently required to dissociate the geminate pair, as shown in Fig. 2.

Thus, ET and the following dissociation reactions are presumed to actually be controlled by different factors in the highly efficient organic photocarrier generating system. In the following section, photoinduced ET and geminate-pair dissociation are discussed regarding the reaction mechanism and the factors controlling it.

Photoinduced Electron Transfer between an Azo Compound and HTM. Based on the scheme in Fig. 6, the preceding ET reaction is controlled by the energy gap, which is defined as the energy difference between the initial and final states. This section describes the energy-gap dependence of ET for photocarrier generation employing 3 azo compounds and 26 HTMs to vary the energy gap over a wide range.

As described in the above section, the CGL of the layered photoreceptor comprises the Azo compound, HTM, and a binder polymer. Thus, the CGL consists of two phases: one is Azo particles, and the other is a solid solution made of HTM and a binder polymer. As shown in Figs. 3 and 7, the ET site is considered to be the Azo/HTM molecular interface, such as a particle/molecularly doped polymer interface.[26] This solid system is assumed to be such as an organic single crystal/adsorbed dye or silver halide microcrystal/adsorbed dye.[27] Therefore, in this extrinsic photocarrier generation system, we can assume that electron transfer occurs from the ionization potential (IP) level of the HTM to the azo compound IP level;[9] hence, the energy gap (ΔE), is presumed to be given by

$$\Delta E = \mathrm{IP(Azo)} - \mathrm{IP(HTM)}. \quad (8)$$

When we use the electrochemical oxidation potential

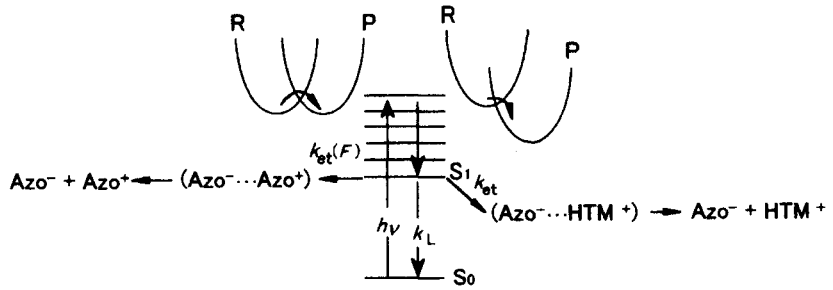

Fig. 6. Schematic of extrinsic photocarrier generation in layered organic photoreceptor and intrinsic one in single-layer CGL. R and P respectively denote reactant and product.

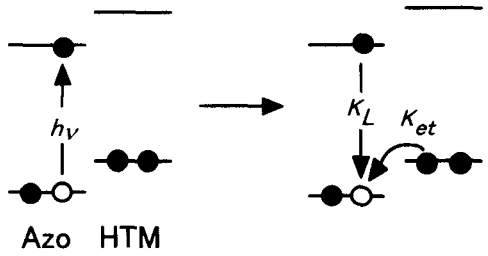

Fig. 7. Schematic energy diagram of the photocarrier generation process at the Azo/HTM interface.

(E_{ox}), which has better reproducibility than IP measured by photoelectron emission spectroscopy, to evaluate the ΔE, a solvation factor cannot be neglected because the following relation exists between the two:[28]

$$IP = E_{ox} + C + E_{solv}. \quad (9)$$

Here, C is a constant and E_{solv} is the solvation energy.

Figure 8 represents the relationship between IP and E_{ox} of three azo compounds and two HTMs shown in Fig. 1. For the oxidation potential, the half-wave potential measured in acetonitrile solution was used for the HTMs, and the peak potential of an ac voltammogram measured by acetonitrile dispersion for azo compounds.[17] The plots in Fig. 8 are linear with a gradient of 1. This implies that the energy gap can be calculated by

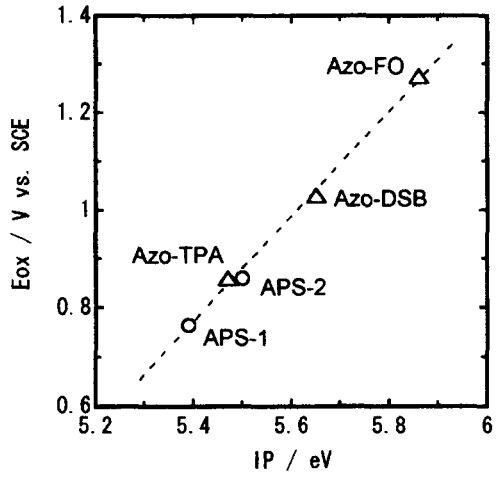

Fig. 8. Ionization potential versus electrochemical oxidation potential of azo compounds and HTMs.

$$\Delta E = E_{ox}(\text{Azo}) - E_{ox}(\text{HTM}). \quad (10)$$

Equation 10 points out that the solvation energy difference between azo and HTM is negligible. This is considered to be a result of nonsolvation for azo compound dispersion and a very small solvation energy for HTM, because the HTM scarcely dissolves in acetonitrile.

Figure 9 shows the relationship between the energy gap defined by Eq. 10 and the quantum efficiency of a layered photoreceptor measured at 3×10^7 V m^{-1} for layered photoreceptors using 3 azo compounds (Azo–FO, Azo–TPA, Azo–DSB) in combination with 26 *N,N*-diphenyl-4-biphenylylamine derivatives (HTMs), shown in Table 1. In Azo–FO, since the dissociation efficiency (ϕ_{diss}), could be taken as 1 at high electric fields (see Fig. 2), the overall quantum efficiency is presumed to be equal to the ET efficiency.[12] Further, we confirmed that the overall efficiencies of many photoreceptors, employing HTMs to vary E_{ox} over a wide range, except for APS-1, were saturated at 3×10^7 V m^{-1}. Moreover, from our preliminary experimental result,[29] our observed Azo–TPA shows the same tendency for the electric-field-dependent PL quenching results as that of Pcs.[25] In this system, as the field is increased, both ϕ and ϕ_{et} increase monotonically and show a linear correlation at a high electric

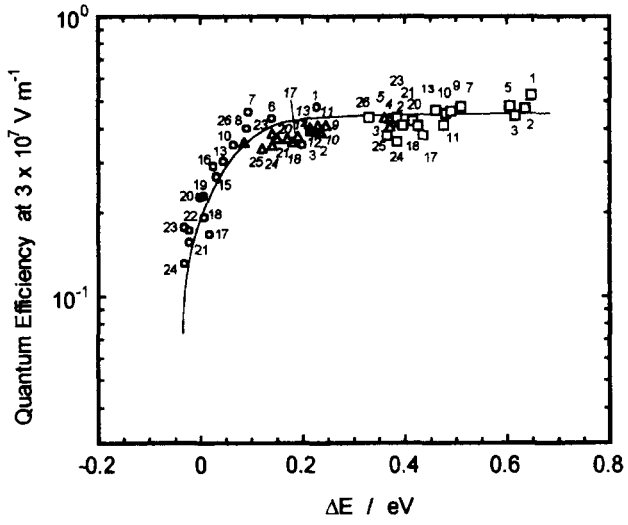

Fig. 9. The energy gap dependence of the quantum efficiency at 3×10^7 V m^{-1}. The numbers in the figure refer to the HTMs used in the CTLs in combination with Azo–FO (squares), Azo–DSB (triangles), and Azo–TPA (circles).

field ($\phi \cong \phi_{et}$). This experimental result could be explained by the field dependence of the preceding photoinduced ET and the following geminate-pair dissociation.[30] This treatment, where the dissociation efficiency equals ca. 1 at a high electric field, is a conventional method in the research field of these solid systems.[7,31,32]

The efficiency shown in Fig. 9 increases according to the increase in the ΔE close to $\Delta E = 0$; this corresponds to the normal region of the Marcus theory.[33,34] However, the overall quantum efficiency is constant for larger ΔE values, even up to values as high as 0.65 eV. Thus, the inverted region is not observed. In contrast, the energy-gap dependence of the quantum efficiency in an oxo(phthalocyaninato)titanium-(IV) (TiOPc)-based layered photoreceptor demonstrates a bell shape,[31] clearly showing a downhill region.[32]

Here, we assume that the Marcus theory is applicable to our layered system; further, we discuss the inverted region in the azo compound-based system in comparison with the phthalocyanine-based system. Under these experimental conditions, the ET efficiency is expressed as[9]

$$\phi_{et} = k_{et}/(k_{et} + k_L), \tag{11}$$

where k_{et} is the electron-transfer rate constant and k_L is the sum of the rate constants of other processes originating in the photoexcited carrier generation material, respectively. The Marcus expression for k_{et} is[35]

$$k_{et} = k_0 \exp[-(\lambda - \Delta E)^2/4\lambda k_B T], \tag{12}$$

where k_0 is the preexponential factor and λ is the total reorganization energy.

Under the assumption $\phi_{diss} = 1$, Eq. 11 is rewritten as

$$k_{et} = k_L \phi/(1 - \phi). \tag{13}$$

Substituting ϕ in Fig. 9 and k_L, which is evaluated as the reciprocal photoluminescence lifetime of the photoexcited single CGL, in Eq. 13, k_{et} was obtained and plotted against the energy gap, as shown in Fig. 10. In this figure, the curves were calculated using Eq. 12. From the figure, the total reorganization energy (λ) is determined to be > 0.4 eV, which is much larger than the values obtained in the solid systems[36] (0.05—0.2 eV).[27] Therefore, the experimental result that the magnitude of k_{et} is constant versus $\Delta E = 0.1$—0.65 eV is concluded to be due to the saturation of k_{et} at large values.

The photoinduced ET for photocarrier generation in azo compound-based photoreceptors is expressed by

$$\text{Azo}^* + \text{HTM} \rightarrow (\text{Azo}^- \cdots \text{HTM}^+). \tag{14}$$

From this expression, the initial and final states of the reaction are neutral and charged, respectively. This is the so-called charge-separation (CS) reaction. The inverted region has not been observed in these CS reactions.[33,34]

Conversely, downhill in the inverted region is apparently certified for a layered photoreceptor containing TiOPc in the CGL. Since TiOPc is known to generate photocarriers

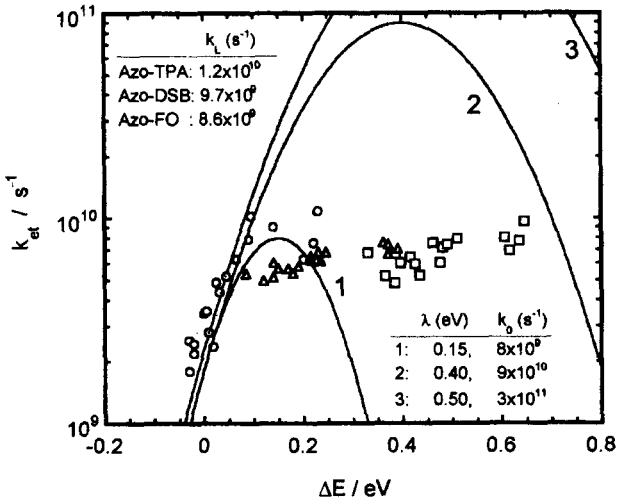

Fig. 10. The energy gap dependence of the ET rate constant. Plots are taken from Fig. 9 using Eq. 13. The curves are the results of calculation based on the Marcus theory with different reorganization energies.

intrinsically,[37,38] the overall quantum efficiency, which depends on HTM,[31] is considered to be governed not by the carrier generating process expressed in Eq. 15a, but by the carrier-injection process given by Eq. 15b:

$$\text{Pc}^* + \text{Pc} \rightarrow \text{Pc}^- + \text{Pc}^+, \tag{15a}$$

$$\text{Pc}^+ + \text{HTM} \rightarrow \text{Pc} + \text{HTM}^+. \tag{15b}$$

The latter hole-injection, rate-determining process, is a charge-shift (CSH) reaction. In such as the CSH reaction, there have been many experimental observations of the inverted region.[33,34]

The two types of ET reaction, CS in the azo-based system and CSH in the TiOPc-based system, well explain the energy-gap dependence of the carrier-generation efficiency in terms of the inverted-region behavior. However, a few models[39,40] explain these experimental results quantitatively.

Conclusions

Studies on extrinsic photocarrier generation in a layered photoreceptor incorporating an azo compound were carried out with a major focus on the reaction steps of photoinduced ET and geminate pair dissociation into free carriers, since the two-step reaction is indispensable for organic materials.

First, the photoinduced ET efficiency and overall quantum efficiency were measured for the layered photoreceptor and the single-layer CGL. The fact that the photoinduced ET efficiency of the layered photoreceptor is much larger than that of the single-layer CGL is presumed to be a result of HTM-enhanced sensitization, which works catalytically to diminish the activation energy for ET. Although such an extrinsic ET takes place independent of an electric field, the following dissociation of geminate pairs depends on the electric field, and is rate determining at lower electric field values.

Next, the preceding ET was investigated in terms of the energy-gap dependence. More than 50 layered photoreceptors were prepared to vary the energy gap over a wide range; the measured efficiency was then plotted against the energy gap, and the inverted region was not observed. This result was explained by charge separation in which an activation energy for ET is almost constant, even at large energy-gap values. In addition, the Marcus inverted region reported for TiOPc-based photoreceptors was considered based on a charge shift-type reaction and compared with the azo-based systems.

References

1 K.-Y. Law, "Handbook of Organic Conductive Molecules and Polymers," ed by H. S. Nalwa, Wiley, Chichester (1997), Vol. 1, Chap. 10.

2 P. M. Borsenberger and D. S. Weiss, "Organic Photoreceptors for Xerography," Marcel Dekker, New York (1998), Chap. 6.

3 J. Simon and J.-J. André, "Molecular Semiconductors," Springer-Verlag, Berlin (1985).

4 R. H. Bube, "Electronic Properties of Crystalline Solids," Academic, New York (1974).

5 A. V. Patsis and D. A. Seanor, "Photoconductivity in Polymers, Technomic," Westport (1976).

6 P. M. Borsenberger and D. S. Weiss, "Handbook of Imaging Materials," ed by A. S. Diamond, Marcel Dekker, New York (1991), Chap. 9.

7 a) Z. D. Popovic and E. R. Menzel, *J. Chem. Phys.*, **71**, 5090 (1979). b) Z. D. Popovic, *J. Chem. Phys.*, **78**, 1552 (1983).

8 M. Umeda, "Trends in Physical Chemistry," Research Trends, Poojapura (1997), Vol. 7, p. 107.

9 M. Umeda, T. Shimada, T. Aruga, T. Niimi, and M. Sasaki, *J. Phys. Chem.*, **97**, 8531 (1993).

10 M. Umeda, T. Niimi, and M. Hashimoto, *Jpn. J. Appl. Phys.*, **29**, 2746 (1990).

11 A. R. Melnyk and D. M. Pai, "Physical Methods of Chemistry," 2nd ed, ed by B. W. Rossiter and R. C. Baetzold, John Wiley and Sons, New York (1993), Vol. 8, Chap. 5.

12 T. Niimi and M. Umeda, *J. Appl. Phys.*, **74**, 465 (1993).

13 L. Sebastian, G. Weiser, G. Peter, and H. Bässler, *Chem. Phys.*, **75**, 103 (1983).

14 M. Umeda and M. Yokoyama, *Jpn. J. Appl. Phys.*, **34**, L44 (1995).

15 a) H. Kirihara and M. Uda, *Rev. Sci. Instrum.*, **52**, 68 (1981). b) K. Yokoyama and M. Yokoyama, *Solid State Commun.*, **70**, 241 (1989).

16 R. O. Loutfy and J. H. Sharp, *J. Appl. Electrochem.*, **7**, 315 (1977).

17 M. Umeda, *Electrophotography*, **27**, 539 (1988).

18 M. Umeda and M. Hashimoto, *J. Appl. Phys.*, **72**, 117 (1992).

19 M. Umeda and T. Niimi, *J. Imag. Sci. Technol*, **38**, 281 (1994).

20 J. Mort and I. Chen, "Applied Solid State Science," ed by R. Wolf, Academic, New York (1975), Vol. 5, p. 83.

21 T. Niimi and M. Umeda, *Adv. Mater.*, **7**, 481 (1995).

22 T. Niimi and M. Umeda, *J. Appl. Phys.*, **76**, 1269 (1994).

23 M. Umeda, T. Niimi, *Jpn. J. Appl. Phys.*, **33**, L1789 (1994).

24 M. Umeda, *J. Imag. Sci. Technol.*, **43**, 254 (1999).

25 Z. D. Popovic, "Proc. 9th International Congress on Advances in Non-Impact Printing Technologies/Japan Hardcopy '93," The Society for Imaging Science and Technology and The Society of Electrophotography of Japan, 1993, Abstr., p. 591.

26 Z. D. Popovic, Ah-M. Hor, and R. O. Loutfy, *Chem. Phys.*, **127**, 451 (1988).

27 For example: a) G. L. Gloss and J. R. Miller, *Science*, **240**, 440 (1988). b) K. Kemnitz, N. Nakashima, and K. Yoshihara, *J. Phys. Chem.*, **92**, 3915 (1988). c) T. Tani, T. Suzumoto, and K. Ohzeki, *J. Phys. Chem.*, **94**, 1298 (1990).

28 J. O'M Bockris and A. K. N. Reddy, "Modern Electrochemistry," Plenum, New York (1970), Vol. 1, Chap. 2.

29 Unpublished results. The details of experiments will be reported elsewhere.

30 M. Umeda, M. Ohta, and M. Yokoyama, "Extended Abstracts (The 44th Spring Meeting)," The Japan Society of Applied Physics and Related Societies, Tokyo, 1997, Vol. 3, p. 1182.

31 C. Randolph and J. Neely, "Proc. IS&T's NIP13: International Conference on Digital Printing Technol.," ed by M. H. Lee, IS&T, Seattle, 1997, p. 274.

32 M. F. Molaire, E. H. Magin, and P. M. Borsenberger, "Organic Photorefractive Materials and Xerographic Photoreceptors," ed by S. Ducharme and J. W. Stasiak, SPIE, San Diego, 1997, SPIE Proc. Series, Vol. 3144, p. 26.

33 M. A. Fox and M. Chanon, "Photoinduced Electron Transfer," Elsevier, New York (1988), Parts A-D.

34 G. J. Kavarnos, "Fundamentals of Photoinduced Electron Transfer," VCH Publishers, New York (1993).

35 a) R. A. Marcus, *J. Chem. Phys.*, **24**, 966 (1956). b) *Annu. Rev. Phys. Chem.*, **15**, 155 (1964).

36 H. Sumi and R. A. Marcus, *J. Chem. Phys.*, **84**, 4894 (1986).

37 a) Y. Fujimaki, "Proc. IS&T's 7th International Congr. Non-Impact Printing Technol.," ed by K. Pietrowski, IS&T, Portland, 1991, Vol. 1, p. 269. b) Y. Fujimaki, H. Tadokoro, Y. Oda, H. Yoshioka, T. Homma, H. Moriguchi, K. Watanabe, A. Kinoshita, N. Hirose, A. Itami, and S. Ikeuchi, *J. Imag. Technol.*, **17**, 202 (1991).

38 A.-M. Hor and Z. D. Popovic, "Proc. IS&T's 7th International Congr. Non-Impact Printing Technol.," ed by K. Pietrowski, IS&T, Portland, 1991, Vol. 1, p. 293.

39 a) T. Kakitani and N. Mataga, *J. Phys. Chem.*, **89**, 4752 (1985). b) *Chem. Phys.*, **93**, 381 (1985).

40 T. Kakitani and N. Mataga, *J. Phys. Chem.*, **90**, 993 (1986).